2015 International Nuclear Atlantic Conference - INAC 2015
São Paulo, SP, Brazil, October 4-9, 2015
ASSOCIAÇÃO BRASILEIRA DE ENERGIA NUCLEAR - ABEN
ISBN: **978-85-99141-06-9**

URANIUM-ZIRCONIUM BASED ALLOYS
Part I: Reference Points for Thermophysical Properties

Marcio Soares Dias[1] and João Roberto L. de Mattos[2]

Serviço de Tecnologia de Reatores – SETRE
Centro de Desenvolvimento da Tecnologia de Nuclear – CDTN
Comissão Nacional de Energia Nuclear - CNEN
CP: 941 - Pampulha
30161-970 Belo Horizonte, MG
[1] marciod@cdtn.br
[2] jrmattos@cdtn.br

ABSTRACT

An integrated modelling process named Relative Variational Model (RVM) is in development by the fuel designers of the CDTN. The lack of measurements in the thermal and physical properties for new fuels, as well as the high dispersion of the existing measurements are challenges in the development of nuclear fuel concepts since that higher uncertainties of the material properties have as result the detrimental reduction on the safety margins . Based on the RVM, the integrated process has been applied to the derivation of reference points for the U-Zr based alloy.

1. INTRODUCTION

Seventy years ago, the first fast breeder reactors, constructed in the 1945-1960 period, used metallic fuels composed of uranium, plutonium, or their alloys. These alloys were chosen because of most existing reactor operating experience had been obtained on metallic fuels and they provided the highest breeding ratios [1].

The potential of a fast reactor (FR) with a closed fuel cycle for breeding fissile isotopes from fertile 238U (or 232Th) and, in turn, exploiting the energy locked in natural uranium, was realized from the very inception of nuclear energy. The present generation of nuclear power reactors use uranium oxide fuel, containing 0.7–5% 235U (the rest being 238U) on a ‘once through’ basis, where only 1% (or even less) of the energy from natural uranium resources are utilized. The rest of the uranium is locked in the tailings of enrichment plants or in spent nuclear fuel. Management of the back end of the nuclear fuel cycle is becoming increasingly important for long-term sustainability of nuclear energy [2].

Operating experience gained with worldwide FR development programs indicated that metal fuel element designs available at the past time could not operate reliably to the high burnups and at the high temperatures as required by power breeder reactors. However, based on the considerable amount of the accumulated experience, demonstrating programs for new designed fuel types including U-Zr and U-Pu-Zr alloys are running since 1990 [1]. By considering this operational experience, the metallic fuel based on the U–Zr alloy is recognized as a promising metallic nuclear fuel in the FR concepts. Furthermore, U rich U-Zr alloys are of interest because of their potential use in low-power or research reactors, since Zr has a low thermal neutron cross-section. Moreover, U-Zr alloy has excellent corrosion resistance and dimensional stability during thermal cycling [3].

In some developed countries, the technology for burning of actinides represents today the mitigation of social and environmental demands in the face of political difficulties with the storage or disposal of spent fuel [2]. So, despite the fact that some specific priorities and demands among the countries may diverge, the accumulated knowledge and positive spin-offs of metallic fuel programs converges to the global interest in the future deployment of nuclear technology as an already available option for Earth's climate future [4]. The Brazilians interests aim social and industrial applications and the use for local electricity generation. One specific interest is related with the once-through fast spectrum systems employing a one-batch fuel management scheme in which the entire reactor core are charged and discharged at the beginning of life (BOL) and end of life (EOL), respectively [5]: one reactor and one core in only one very long residence time. The accurate knowledge of the thermophysical properties of the U-Zr alloys as a function of temperatures and other parameters is essential for the development of the **all-metal reactor concept**. Nevertheless, experimental data on these properties are yet scarce [6]. The lack of measurements of the material properties for new fuels is a problem in the development of advanced concepts and, as consequence; the safety margins[1] in the design are reduced.

Nuclear fuel designers must demonstrate the safety of the reactor by detailed examination of the outcome from postulated steady state and transient operational conditions. By seeking the development of new generators, other than the uranium oxide, uranium alloys are promising as nuclear fuel, since these alloys achieve both higher uranium densities and extended fuel burnup. Effective heat removal from the fuel elements poses as one of the primary considerations in reactor design, and the knowledge of thermophysical properties of the materials is essential for the design of new nuclear fuels. Density and thermal expansion, specific heat, thermal conductivity and diffusivity are primary properties in the design calculations of fuel elements. However, thermophysical data of U-Zr based alloys and, in special, of the U-Zr-Nb alloy, are scarce and disperse, presenting large uncertainties. Uncertainties in a property contribute to detrimental reduction of the safety margins in the fuel element design.

Currently, experimental data of the U-Zr alloy from the open literature are being revised and reduced by applying the Relative Variational Model to depict the dependences of the thermal properties on the entire composition range, on the temperature range from 0 K up to the melting point and, at the same time, to derive integrated estimates of the associated uncertainties. The U–Zr alloy is recognized as a promising metallic nuclear fuel that can attend the Brazilian future use of the nuclear energy in the social and industrial applications and for local electricity generation. Model validation for data reduction and significant reductions of the uncertainties are obtained in the data evaluation[2] and are summarized in the present paper.

2. HISTORY AND PERSPECTIVES OF THE FUELS FOR FAST REACTORS

Kittel et al. [1] in the “History of fast reactor development” presented in 1993 an overview of the nuclear fuel development. After this paper, fifty years of FR fuel element development have seen fluctuations in the popularity of the various fuel types from Fermi’s initial use of

[1] Safety margin means here the withstand excess of a design limit up to the failure.

[2] Data evaluation follows NIST recommendations [9]. Software “Plot-digitizer” [10] was applied for data collection from figures. Software “Table Curve 3D” was used for data reduction and statistics [11].

oxide in CP-1, the first reactor, to emphasis on metal fuels, thence to ceramics, and finally back to both ceramic and metal as performance demands and priorities have changed. The history of fast experimental reactors is very close to the history of the nuclear fuels development as they were the tools for the demonstrating programs of the nuclear materials.

Difficulties in obtaining adequate dimensional stability in metallic fuel elements under conditions of high fuel burnup led in the 1960s to the virtual worldwide choice of ceramic fuels. Although ceramic fuels provide lower breeding performance, this objective is no longer an important consideration in most national programs. Mixed uranium and plutonium dioxide became the ceramic fuel that has received the widest use. More advanced ceramic fuels like mixed uranium and plutonium carbides and nitrides are under slow development. However, the critical factor that will make fast reactors competitive with thermal reactors is fuel burnup - doubling burnup nearly halves the fuel cycle cost and greatly reduces electrical generation costs. Thus, a major thrust since the 1970s has been to achieve high fuel burnups - 20 at%[3] is typically a current objective.

In a subsequent development phase, metallic fuel elements of improved design have joined ceramic fuels in achieving goal burnups of 15 to 20 at% (140 to 190 MWd/kHM). Low-swelling alloys for the fuel cladding have also been continuously developed. It is the cladding material that has perhaps had the greater influence on the course of fuel rod development as the true effects of fast neutrons on cladding alloy properties have been uncovered. Anyway, basic science has made its contribution to the understanding of radiation effects in the cladding and fuel materials, and the goals of the designers were attained in terms of burnup and core residence time [1].

Uranium proved to be much more abundant than originally imagined and, after a fast start, nuclear power growth slowed dramatically in the late 1980s and, the global nuclear capacity is today about one-tenth of the level projected in the early 1970s. The urgency of deploying fast reactors for plutonium breeding therefore abated in the western OECD countries. However, in India and Russia, concerns about potential near-term uranium shortages persist, and new demonstration breeder reactors are being built. China is building two Russian-designed breeder reactors [13]. Chinese Demonstration Fast Reactors had scheduled commissioning to 2018-19.

Interest in fast-neutron reactors persists in some OECD countries, but, for a new reason: the political difficulties with storing or disposing of spent fuel. “Reprocessing” of the spent fuel does not eliminate the problem of siting a geological repository but a reprocessing plant does provide an interim destination that has proved a path forward with regard to the spent fuel problem in a number of nations [13].

The renewed interests in the FRs in the last years are summarized by references [2, 12, 14-18]. Kim and Taiwo [5] evaluated the fuel cycle characteristics of once-through nuclear systems. In this evaluation the uranium utilization for some reactor cycle systems have also been compared. In the PWR systems, the uranium utilization is less than 1 at% regardless of the burnup and for the once-through fast spectrum systems; the uranium utilization could be increased to ~30 at%, depending on the core design. However, some technical design issues

[3] Burnup is here reported using either at% or GWd/MTHM (=MWd/kHM), consistent with the units used in the bibliographic sources: 1 at% of burnup is roughly 9.4 GWd/MTHM [12].

must be resolved before these concepts begin to be practical. The issues are related to ultra-high burnup fuel, extremely long life of the reactor in order to get effective breeding and burnup, the core system size must be large, and difficulties can be anticipated for the power and reactivity controls.

The best neutronic performance characteristic of the metallic fuel enables core designs with minimum burnup reactivity swing even for small modular designs. This can be used not only for extending the core life up to 30 years but also in reducing the transient overpower without scram (TOPWS), which can be initiated by unprotected run out of the control rod. Transient overpower tests on metallic and oxide fuels performed in Transient Reactor Test Facility demonstrated a larger margin to cladding failure threshold of the metallic fuel in relation to the oxide fuel. Oxide fuel pins fail typically 2.5–3 times nominal peak power (4–4.5 times in adiabatic conditions), whereas metallic fuel pins fail 4–4.5 times nominal peak power [19].

3. METALLIC NUCLEAR FUEL EXPERIENCE

The US experience with oxide, metal, and carbide fuels is substantial, comprised of irradiation of over 50.000 MOX rods, over 130.000 metal rods, and 600 mixed carbide rods, in the EBR-II (Experimental Breeder Reactor) and FFTF (Fast Flux Test Facility) [12]. All three types have been demonstrated capable of fuel utilization at or above 21 at% (200 MWd/kHM). Life-limiting phenomena for each type have been identified and investigated, and there are no disqualifying safety-related fuel behaviors. Improvements in irradiation performance of cladding and duct alloys were a key development in moving these fuel designs toward higher-burnup potential [12].

Metallurgists had recognized in the 1950s that α-uranium alloys would quite likely not enable goal burnups of several atom percent to be achieved. Metastable γ-uranium alloys appeared to provide the best solid metallic fuel material that would be resistant to both irradiation growth and swelling. Uranium alloy containing 10 wt% molybdenum offered the most promise, and it was chosen for intensive development in several countries including France, the Russia, the UK, and the US. However, instability was observed and attributed to the thermally-induced transformation of the γ–phase to the α+δ–phases, and the irradiation-induced reversion of this transformation to the more desirable γ–phase [1]. The unusual irradiation growth and swelling exhibited by some alloys were attributed to textured microstructural phases with anisotropic crystal structure resulting from fabrication. Heat treatment was applied to the as-fabricated fuel in order to remove crystallographic texture and to stabilize predominantly isotropic crystal structures at irradiation temperatures [12].

Aiming to avoid excessive fuel swelling and based on results from irradiation studies, the fuel alloy should not exceed the temperature of 650°C or operate in the 480-580°C temperature range at fission rates below 8 x 10^{13} fissions/cm^3s [1]. The Mark III fuel elements[4] were operated reliably throughout the life of the Dounreay Fast Reactor under the above conditions and the cladding temperature criterion of 480°C [1].

Main solutions to the above-mentioned constraints were addressed with changes of the fuel rod design. These changes were embodied in the Mark-II fuel design and they included (a) addition of impurity-level amounts of Si to reduce the rate of the fuel swelling, (b) larger

[4] Mark fuel elements are designs used in demonstrating programs of the Experimental Breeder Reactor (US) and Dounreay Fast Reactor (UK) [1, 12, 15, 19, 20]

fuel-to-cladding gap to accommodate swelling until the point where the interconnection of the fuel porosity takes place and the fission gas is released into the fuel plenum, (c) larger fuel plenum to accommodate the released fission gas, and (d) thicker cladding wall. The cladding alloy was later changed to improve the swelling resistance and to mitigate fuel-cladding interdiffusion (which reduces the load-bearing thickness of the cladding wall) [12].

As key to obtaining high burnups in metal fuels it was allowed the fuel to swell approximately 30% within its cladding [1]. At that point, the fission gas bubbles become largely interconnected to the fuel surface and the volatile fission products are directly released into the fuel element plenum. In addition, the resulting porous fuel is mechanically weak and can be restrained by relatively thin cladding [1].

An experimental program was undertaken to adapt principles learned in evolution of EBR-II fuel design to U–Pu–Zr, for varying amounts of Pu. These experiments demonstrated burnup potential of U–19Pu–10Zr and U–10Zr fuels and clad in advanced alloys near 20 at%, the burnup level that had become a goal of the US fast reactor program as part of an effort to make fast reactor fuel cycles competitive with light water reactor fuel cycles [12].

Although the metal fuel melting temperature is much lower than that of oxide fuel, it is also much more difficult to raise the fuel temperature because of the high thermal conductivity (~20 W/mK for metal compared to ~2 W/mK for oxide). As a result, operating margins in terms of power can in fact be greater for the metal core than for oxide core [19]. Metal fuel provides better or equal safety characteristics under the entire operational spectrum of the normal behavior up to postulated severe accidents. However, it is in the inherent passive safety characteristics under the generic anticipated transient without scram events, such as loss-of-flow without scram (LOFWS), loss-of-heat-sink without scram (LOHSWS), and transient overpower without scram (TOPWS), that the metal fuel shows its greatest advantages over oxide fuel. The inherent passive safety potential of the metal fuel has been demonstrated by two landmark tests conducted in EBR-II on April 3, 1986 [19].

One approaches pursued to solve the fuel/cladding compatibility problem included alloy additions, mainly to U-Pu fuel alloys. Ternary U-Pu alloys were investigated in the USSR, France, the UK, and the US. The alloy additions investigated most extensively included Mo, Nb, Ti, Zr, and Fs (Fissium)[5], of which Zr was found to be the most effective [1]. Zirconium was chosen as an alloying element for metallic fuels since it increases the solidus temperature. It also helps in overcoming the fuel clad chemical interaction and helps in stabilizing the isotropic γ-phase over a wider temperature range. Uranium alloyed with Zr has excellent dimensional stability during thermal cycling [22].

4. URANIUM-ZIRCONIUM SYSTEMS

The equilibrium U-Zr phase diagram of the Fig. 1 shows the rising of the melting temperatures in function of the zirconium content. Table 1 summarizes the special points in this diagram. As previously indicated the promising use of the U-Zr or U-Zr-Nb alloys is the stabilized gama phase below of the limit temperature for phase transition of 890 K (617^{o}C).

[5] Fissium (Fs) is an equilibrium concentration of fission product elements left by the pyrometallurgical reprocessing cycle designed for EBR-II and consists of 2.4 wt% Mo, 1.9 wt% Ru, 0.3 wt% Rh, 0.2 wt% Pd, 0.1 wt% Zr, and 0.01 wt% Nb [21]. It is a simulated mixture of noble metal fission products [22]

Fabrication tests have been conducted in the CDTNs to produce the γ-phase of the U-Zr-Nb alloy which attends the prior mentioned metallugical requirements. Results of the fabrication process are given in the references [24-26]. The CDTNs fuel designers are just initiating the evaluations in order to obtain a metallic core concept and the design specifications for the fuel element.

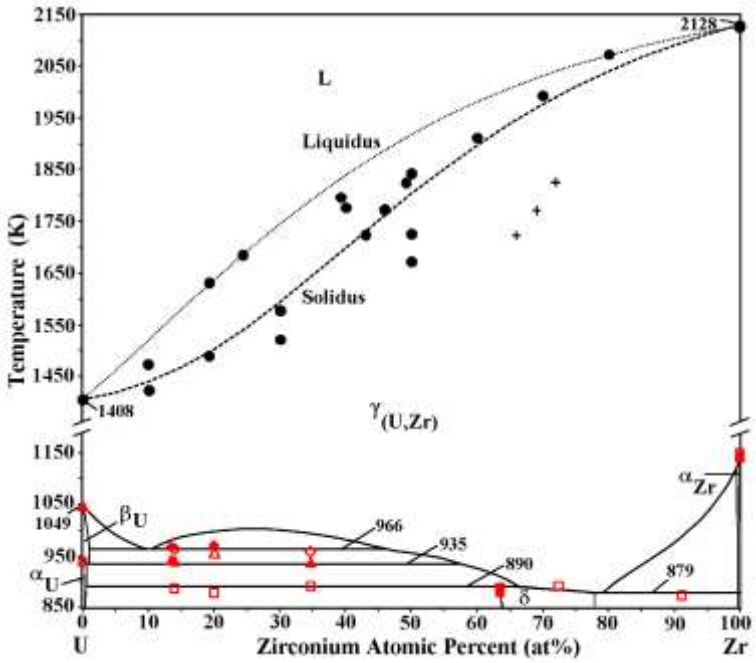

Figure 1: Phase diagram of the Uranium-Zirconium System [23**].**

Table 1: Special Points of the U-Zr Phase Diagram [23**].**

Reaction	Composition of the respective phases, at% Zr			Temperature, K	Reaction Type
L↔U	0			1408	Freezing point
γU↔βU	0			1049	Allotropic transformation
βU↔αU	0			942	Allotropic transformation
γ1↔γ2+βU	10.9	42.4	1.1	966	Monotectoid
βU↔αU+γ2	0.8	0.5	60	935	Eutectoid
αU+γ2↔γ	~0.5	~66	63	890	Peritectoid
γ2↔γ+αZr	~81	~78	99.6	879	Eutectoid
L↔βZr	100			2128	Freezing point
αZr↔ βZr	100			1135	Allotropic transformation

4.1. Density and Thermal Expansion of Pure Elements U, Zr and Nb and alloys

The specific masses and lattice parameters of the pure components in the U-Zr-Nb alloy have been revised and are presented in Table 2. Fig. 2 and Table 3 show the RVM fitting to the mean atomic volume in the α– and γ–phases of the U-Zr alloy in function of the Zr content **x**. In the fit of the α–phase were used the 28 measurements of pure Uranium, 19 of pure Zirconium and 32 of the U-Zr alloy. Previously, 6 measurements of the U-Zr alloy were discharged under the criterion of large deviation in the basic evaluation process [9]. Elias and Dias [27] give details of the data evaluation and 36 references, sources of the 59 experimental values for the all U and Zr phases**.** The data of the U-Zr alloy are from references [3, 28-33].

Table 2: Data of the pure components at room temperature

Phase	Structure	Specific Mass	Atomic Volume	Lattice Parameter
		$\rho\pm\sigma$ (g/cm^3)	$V\pm\sigma$ (Å^3)	a, b, c $\pm\sigma$ (Å)
Uranium				
α	Orthorhombic	19.05±0.02	20.75±0.02	a=2.8536±0.0007
				b=5.8687±0.0024
				c=4.9557±0.0030
β	Tetragonal	18.77±0.02	21.06±0.02	a=10.5890±0.0033
				c=5.6339±0.0039
γ	Body centered cubic	18.62±0.15	21.23±0.17	a=3.4884±0.0091
Zirconium				
α	Hexagonal	6.502±0.004	23.29±0.01	a=3.2328±0.0007
				c=5.1481±0.0012
β	Body centered cubic	6.590±0.008	22.98±0.02	a=3.5822±0.0012
Niobium				
α	Body centered cubic	8.582±0.004	17.976±0.001	a=3.3005±0.0005

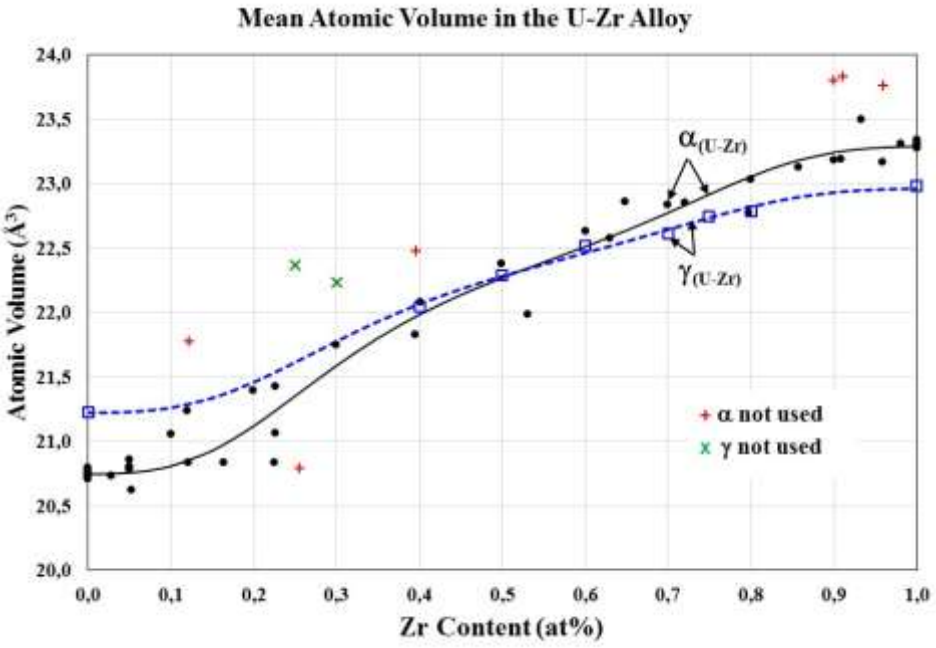

Figure 2: Mean atomic volume in the α- and γ-phases of the U-Zr Systems

The RVM is given by the equation:

$$\mathbf{V(x) = V_{phase_{(U_{1-x}Zr_x)}} = V_{phase_U} . f_0 . (1 + F_U + F_{Zr})} \qquad (1)$$

where

i) $\mathbf{V_{phase_U} = V_{phase}(x = 0)}$ is the volume of the pure U in the α- or γ-phase given in Table 2;

ii) $\mathbf{F_U = \frac{a_1 \cdot \left(\frac{x}{a_0}\right)^3}{\left[1+\left(\frac{x}{a_0}\right)^3\right]}}$ is the component due to the U-atom vibrations in the U-Zr matrix;

iii) $F_{Zr} = \frac{a_2}{\left[1+\left(\frac{1-x}{a_0}\right)^3\right]}$ is the component due to the Zr-atom vibrations in the U-Zr matrix;

iv) $f_0 = \frac{1+a_0^3}{a_0^3.(1+a_2)}$ is the normalization factor for the Uranium atomic volume at $x = 0$;

v) a_0, a_1 and a_2 are adjustable parameters (a_0 characteristic Zr content, a_1 and a_2 are the contribution factors of the U- and Zr-atom vibrations in the U-Zr matrix).

Fig. 3 and Table 3 show the mean atomic volume in the U-Nb system, using 29 measurements from a total of 31 results, according to the references [34-37]. In this case, however the equation is given by:

$$V(x) = V_{phase_{(U_{1-x}Nb_x)}} = a_3.(1 + F_U + F_{Nb}) \quad (2)$$

where a_0, a_1, a_2 and a_3 remain as adjustable parameter, a_1, and a_2 are negative parameters to represent the atomic volume reduction in function of the Nb content, and $a_3 = V_{phase_U}$ is left to be adjusted from the available experimental data of the U-Nb system. In the U-Nb systems, M. Anagnostidis et al. [34] observed the structures α (orthorhombic), α' (orthorhombic) and α'' (monoclinic) for $0 \leq x_{Nb} \leq 0.16$ and γ (tetragonal) for $0.16 < x_{Nb}$. All results from these structures are plotted in the Fig. 3.

Table 3: Adjusted parameters and statistics from the data reduction of the α and γ phases of the $U_{1-x}Zr_x$ alloy and $Nb_{1-x}Zr_x$ alloy

Alpha Phase $U_{1-x}Zr_x$					
R^2 Coef. Det.:		0.99048	**Fit. Standard Error:**		0.1126
Parm	**Value**	**Std Error**	**95% Confidence Limits**		**P > |t|**
a_0	0.044	0.004	0.036	0.052	0.00000
a_1	0.314	0.015	0.284	0.345	0.00000
a_2	0.0825	0.0036	0.0753	0.0897	0.00000

Gamma Phase $U_{1-x}Zr_x$					
R^2 Coef. Det.:		0.99905	**Fit. Standard Error:**		0.0248
Parm	**Value**	**Std Error**	**95% Confidence Limits**		**P > |t|**
a_0	0.027	0.002	0.024	0.031	0.00000
a_1	0.333	0.013	0.304	0.362	0.00000
a_2	0.0581	0.0015	0.0548	0.0615	0.00000

Alpha Phase $U_{1-x}Nb_x$					
R^2 Coef. Det.:		0.99749	**Fit. Standard Error:**		0.0703
Parm	**Value**	**Std Error**	**95% Confidence Limits**		**P > |t|**
a_0	0.081	0.007	0.067	0.096	0.00000
a_1	0.36	0.03	0.298	0.423	0.00000
a_2	0.0601	0.0069	0.046	0.0742	0.00000
a_3	20.95	0.04	20.86	21.03	0.00000

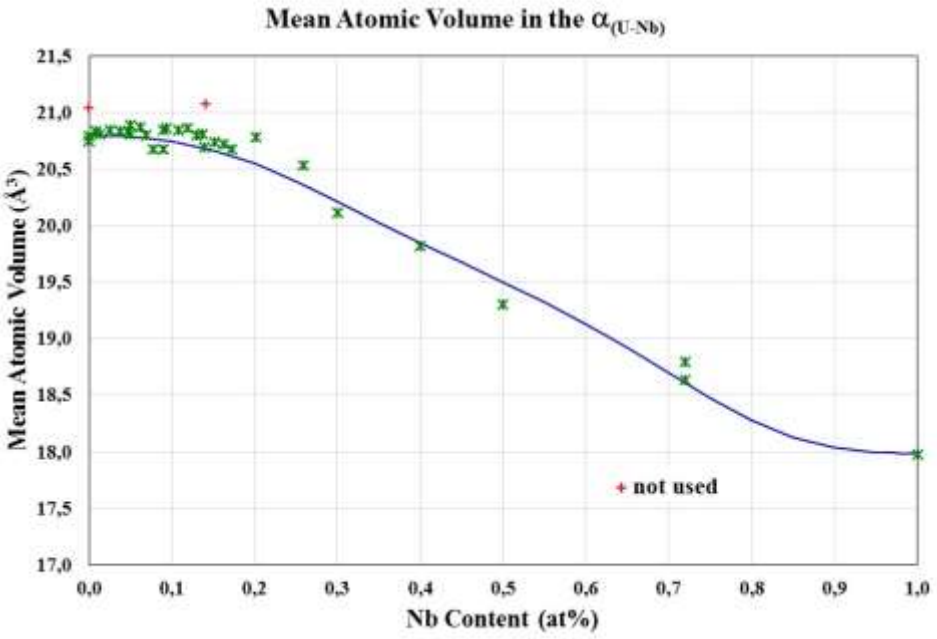

Figure 3: Mean atomic volume in the α-phase U-Nb System

All fittings in the Fig. 2 and 3 attend the conditions $\frac{dV}{dx} \to 0$ and $\frac{d^2V}{dx^2} \to 0$ as $x \to 0$ (pure Uranium) and $x \to 1$ (pure Zirconium or pure Niobium).

The uranium specific mass calculated from the adjusted atomic volume $a_3 = V_{\alpha_U}$ = 20.95 Å^3 has the value of 18.87 g/cm^3, which diverges in –1% from the value 19.05 g/cm^3 (mean value from 28 measurements at room temperature).

Data reductions for the thermal expansions of pure Uranium, pure Zirconium and the existing data for U–Zr and U–Zr–Nb alloys are next steps in order to derive the estimates and uncertainties of the specific mass in function of the composition and temperature. Linear thermal expansion coefficient of pure Niobium based on 562 experimental results [38-55] is illustrate in the Fig. 4. From this amount, 20 measurements (3.6% of the total) were discharged under the criterion of large deviation in the basic evaluation process. The fit of the RVM is obtained in the entire range of temperature by means of 4 components (RVM = F1+F2+F3+F4) with 2 adjustable parameter each, excepted the component F4 where the characteristic temperature is related with the melting temperature of Niobium by means of the equation $T_4 = \left(\frac{1}{2}\right)^{(1/3)} . T_{melting}$. The general form of RVM is given as:

$$RVM = \alpha(T) = \sum_{i=1}^{4} Fi = \sum_{i=1}^{4} \frac{a_i . \left(T/T_i\right)^{\beta}}{\left[1 + \left(T/T_i\right)^{\beta}\right]} \qquad (3)$$

where a_i is the contribution of each vibration mode **i** to the linear thermal expansion coefficient α, T_i is the characteristic temperature of the vibration mode **i**.

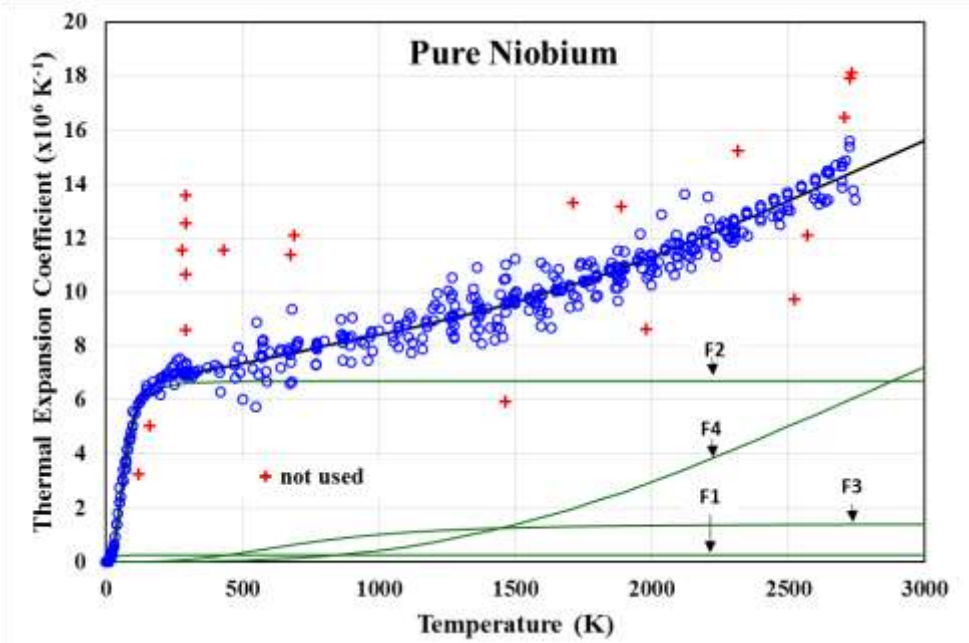

Figure 4: Data reduction of the linear thermal expansion coefficient of the pure Niobium

4.2. Specific Heat of Pure Elements U, Zr and Nb and alloys

Data evaluation of the specific heats at constant pressure, $\mathbf{C_p}$, are almost concluded for pure Uranium, Zirconium and the U–Zr alloy. The fit of the RVM to the data of the U-14%Zr alloy is given in Fig. 5. The data reductions involved 1944 measurements and 79 results (4.1% of the total) were discharged under the criterion of large deviation in the basic evaluation process. Lopes Jr. and Dias [56] present the details of this work and the 35 references, which are sources of the data. The applied RVM to fit the data has the general form:

$$\left(\frac{c_p}{6.R}\right)_{U_{(1-x)}Zr_x} = g_0^s\left(A_0.F_\alpha + F_{tr1} + F_{tr2}\right) + g_{ht}^s.F_{ht} \tag{4}$$

$$g_0^s.A_0.F_\alpha = g_0^s.A_0.\left((1-x).\left(\frac{c_p}{6.R}\right)_{\alpha U_2} + x.\left(\frac{c_p}{6.R}\right)_{\alpha Zr_2}\right) \tag{5}$$

where $g_0^s.A_0.F_\alpha$ is the specific heat of the U-Zr alloy by applying the Neumann-Koop rule; $\left(\frac{c_p}{6.R}\right)_{\alpha U_2}$ and $\left(\frac{c_p}{6.R}\right)_{\alpha Zr_2}$ are the specific heat of the pure Uranium and pure Zirconium, respectively; $\mathbf{R}$ is the universal gas constant, F_{tr_j} represents the pre-transition effects depicted by a half peak with maximum at the phase transition temperatures T_{tr_j}, and $F_{ht} = A_{ht}.g_{ht}^s.e^{-x/3.1}$ is an empirical factor to fit the data in the gamma phase, $g_{ht}^s = 1$ for temperatures below the transition temperature, otherwise $g_{ht}^s = 0$.

The specific heats of pure U and pure Zr have the general form given by the equation (3), and F_{tr_j} is transitory function given by the derivative:

$$F_{trj} = \left(\frac{d\alpha}{dT}\right)_j = g_j\left(T_{trj}\right).\frac{3.a_j}{T_j}\left(\frac{\left(T/T_i\right)}{1+\left(T/T_i\right)^\beta}\right)^2 \tag{6}$$

where $g_j = 1$ for $T \le T_{trj}$, otherwise $g_j = 0$ for $T > T_{trj}$ and T_{trj} is temperature at the phase transition j ($\alpha \leftrightarrow \beta$ or $\beta \leftrightarrow \gamma$) given in the Fig. 1 and Table 1.

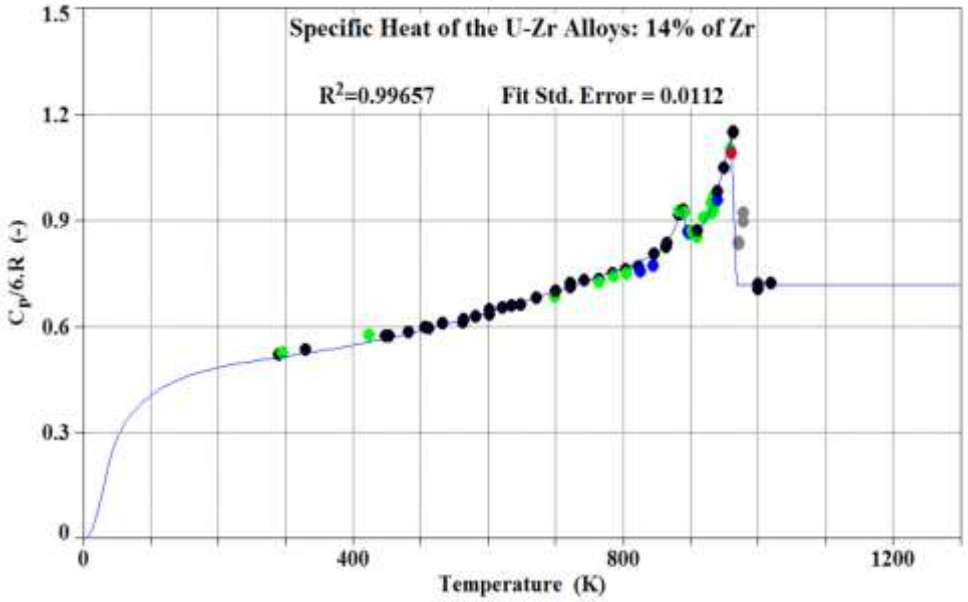

Figure 5: Data reduction of the specific heat of the U-14%Zr alloy [56]

The validity of the Neumann-Koop rule is given by A_o = 1 in the equation (5). The adjusted values of A_o for 5 compositions of U-Zr alloys are presented in the Fig. 6. The pre=exponential term A_{ht} is constant for the compositions used in the data reduction. The empirical relationship $F_{ht} = A_{ht} \cdot g_{ht}^{s} \cdot e^{-x/3.1}$ allows the specific heat in the gamma phase to be evaluated in function of the Zr content **x**.

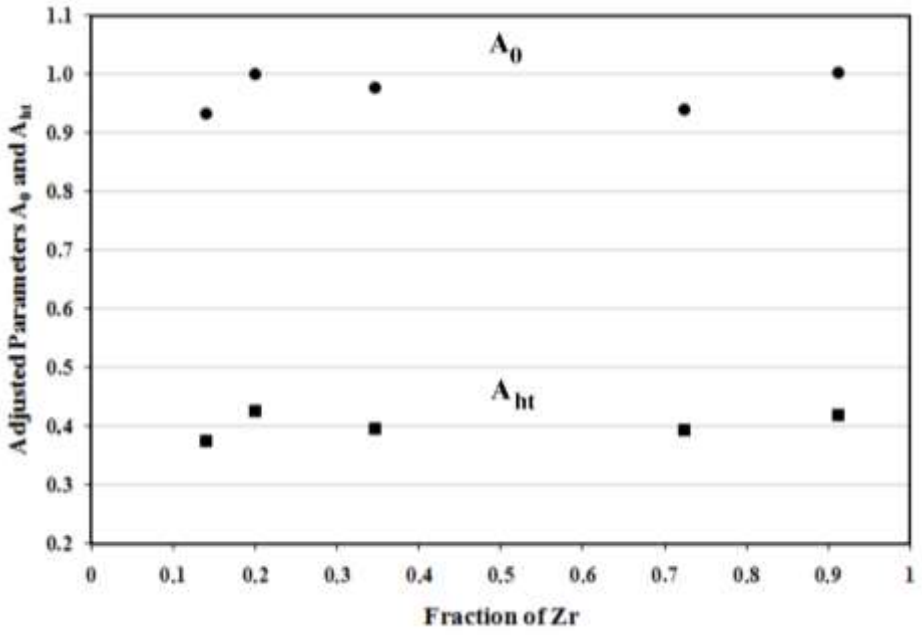

Figure 6: Validity of Neumann-Koop rule ($A_0 \approx 1$) and value of the pre-exponential factor A_{ht} for the specific heat in the gamma phase [56]

4.3. Thermal conductivity and diffusivity of U, Zr and Nb and alloys

The thermal conductivity **k**, thermal diffusivity δ, density ρ (= thermal expansion) and the specific heat at constant pressure $\mathbf{C_p}$ are interdependent properties according to the equation:

$$\mathbf{k = \delta.\rho.C_p} \tag{7}$$

The product $\mathbf{\rho.\ C_p}$ allows the ratio **k/δ** to be evaluated. The thermal property $\mathbf{\rho.\ C_p}$ can be used as reference filter to discharge highly dispersed values in the **k=k(x,T)** and **δ=δ(x,T)** results. Evaluation of **k=k(x,T)** or **δ=δ(x,T)** data, jointly with the $\mathbf{\rho.C_p}$ results, enlarges the database of the U-Zr and U-Zr-Nb and, statistically, reduces the uncertainties relative to the alloy properties. As illustration, Fig. 7 [27] shows the $\mathbf{\rho.C_p}$ data of pure Uranium at low temperatures $\mathbf{0 \le T \le T_{room} = 298\ K}$ and the $\mathbf{k/\delta}$ results at temperatures above of $\mathbf{T_{room}}$. The dispersion of the $\mathbf{\rho.C_p}$ data is clearly smaller than dispersion of the **k/δ** property.

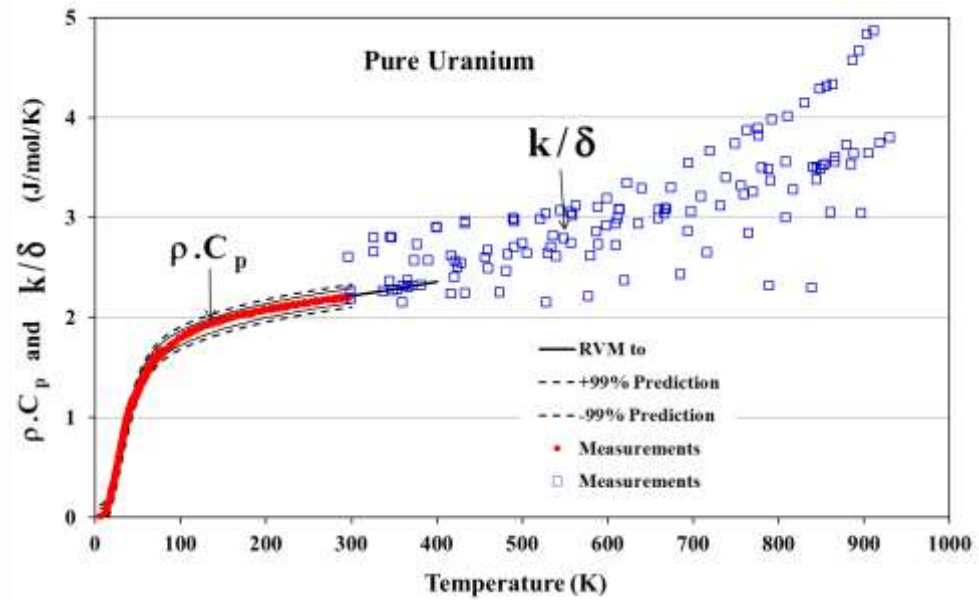

Figure 7: $\mathbf{\rho.C_p}$ (low temperature) and $\mathbf{k/\delta}$ (high temperature) for pure Uranium [27]

5. CONCLUSIONS

By considering the Brazilian potential needs in the future use of the nuclear energy, which can attend the social or industrial demands as well as demand for local electricity generation, an integrated modelling process is in development by the fuel designers of the CDTN addressed to new fuel for all-metal reactor concept.

The lack of measurements of the thermal and physical properties for new fuels, as well as the high dispersion of the existing measurements are challenges in the development of advanced concepts since that higher uncertainties of the material properties have as result the detrimental reduction on the safety margins. Based on the Relative Variational Model this integrated process makes it possible to evaluate key design properties for less-known material by considering the existing knowledge from the pure components. Up to now, the model has been successful applied in the modeling the thermal and mechanical properties of ceramics (Al_2O_3, UO_2 and $(U,Gd)O_2$). The modeling of metallic fuel is just at the beginning, and the current stage of development was presented herein.

ACKNOWLEDGMENTS

This research project is supported by the following Brazilian institutions: Nuclear Technology Development Center (CDTN), Brazilian Nuclear Energy Commission (CNEN), Research Support Foundation of the State of Minas Gerais (FAPEMIG), and Brazilian Council for Scientific and Technological Development (CNPq).

REFERENCES

1. J.H. Kittel et al., "History of fast reactor fuel development", *J. of Nuclear Materials*, **204**, pp.1-13, (1993).
2. International Atomic Energy Agency, "Status of developments in the back end of the fast reactor fuel cycle", *IAEA nuclear energy series*, **STI/PUB/1493**, 103 p., (2011).
3. C. Basak et al., "An evaluation of the properties of as-cast U-rich U–Zr alloys", *J. of Alloys and Compounds*, **480**, pp.857–862, (2009).
4. M.S. Dias and J.R.L. de Mattos, "Human race actions versus the breaking of the CO_2 equilibrium limit", *INAC*, Belo Horizonte, MG, Brazil, October 24-28, (2011).
5. T. K. Kim and T. A. Taiwo, "Fuel cycle analysis of once-through nuclear systems", Argonne Nat. Lab., http://www.ipd.anl.gov/anlpubs/2010/09/67863.pdf (accessed in May 2015), 57 p., (2010).
6. Y. Takahashi, M. Yamawaki and K. Yamamoto, "Thermophysical properties of the Uranium-Zirconium alloys", *J. of Nuclear Materials*, **154**, pp.141-144, (1988).
7. M.S. Dias; V. Vasconcelos; J.R.L. Mattos and E. Jordão. "The Relative Variational Model - A topological view of matter and its properties", paper **406**: "**space occupancy by the atoms",** paper **324**: "**specific heat and enthalpy"**, paper **404**: "**thermal expansion**", *PHYSOR 2012*, Knoxville, Tennessee, US, April 15-20, 2012, CD-ROM, American Nuclear Society, (2012).
8. M.S. Dias, V. de Vasconcelos, J.R.L. de Mattos, F.S. Lameiras, E. Jordão. "The Relative Variational Model: A topological view of matter and its properties", paper **405**: "**$UO_{2\pm x}$ density"**, *PHYSOR 2012*, Knoxville, Tennessee, US, April 15-20, 2012, CD, ANS, (2012).
9. R.G.Munro, "Data Evaluation - Theory and Practice for Materials Properties". NIST recommended practice guide, Washington, June 2003, 114 p. (*Special Publication 960-11*).
10. "Plot Digitizer", Department of Physics, South Alabama University, (Accessed in 2014) http://www.southalabama.edu/ colleges/artsandsci/physics/software.html,
11. "TABLE CURVE 3D**"**, SYSTAT Software Inc., Richmond, CA, US, (2002).
12. D. C. Crawford, D. L. Porter and S. L. Hayes, "Fuels for sodium-cooled fast reactors: US perspective", *J. of Nuclear Materials*, **371**, pp.202-231, (2007).
13. F. von Hippel, "Overview: The Rise and Fall of Plutonium Breeder Reactors", pp.1-15, IN: T. B. Cochran et al., "Fast Breeder Reactor Programs: History and Status", Research Report 8, *2010 International Panel on Fissile Materials*, (Feb. 2010), (accessed in May 2015) http://fissilematerials.org/library/2010/02/fast_breeder_reactor_programs_.html
14. American Nuclear Society, Position Statement: (**ANS-56-2005**) "Need for Near-Term Deployment", (**ANS-74-2005**) "Fast Reactor Technology: A Path to Long-Term Energy Sustainability", (**ANS-75-2005**) "The Need for Deployment of the Next Generation Nuclear Plant Project" and (**ANS-79-2006**) "International Cooperation for Expansion of Nuclear Energy", http://www.ans.org/pi/ps/ (accessed in May 2015)
15. D.E. Burkes et al., "A US perspective on fast reactor fuel fabrication technology and experience. part I: metal fuels and assembly design", *J. of Nuclear Materials*, **389**, pp.459-469, (2009).
16. T. B. Cochran et al., "Fast Breeder Reactor Programs: History and Status", Research Report 8, *2010 International Panel on Fissile Materials*, (Feb. 2010), (accessed in May 2015). http://fissilematerials.org/library/2010/02/fast_breeder_reactor_programs_.html

17. H. S. Khalil, “Fast Reactor Development: Motivation, Challenges and Recent Advances”, ANL, http://www.nremp.gatech.edu/files/ne50/presentations/NE50_8_Khalil.pdf (accessed in May 2015)
18. T. Sathiyasheela et al., “Inherent safety aspects of metal fuelled FBR”, *Nuclear Engineering and Design*, **265**, pp.1149-1158, (2013)
19. Y. I. Chang, “Technical rationale for metal fuel in fast reactors”, *Nuclear Eng. and Technology*, **39(3)**, pp.161-170, (2007).
20. C.E. Lahm et al., “Experience with advanced driver fuels in EBR-II”, *J. of Nuclear Materials*, **204**, pp.119-123, (1993).
21. L.C. Walters, “Thirty years of fuels and materials information from EBR-II”, *J. of Nuclear Materials*, **270**, pp.39-48, (1999).
22. S. Kaity et al., “Microstructural and thermophysical properties of U–6 wt%Zr alloy for fast reactor application”, *J. of Nuclear Materials*, **427**, pp. 1–11, (2012).
23. R.I. Sheldon and D.E. Peterson. “The U-Zr (Uranium-Zirconium) System”, *Bulletin of Alloy Phase Diagrams*, **10(2)**, pp. 165-71, (1989).
24. D. M. Camarano et al., “Thermophysical Properties of Uranium-Based Niobium and Zirconium Alloys from 23 ^{o}C to 175 ^{o}C”, *Int J. Thermophys.*, **31**, pp.1842–1848, (2010).
25. N. M. Cantagalli and W B. Ferraz, “Desenvolvimento do combustível tipo placa da liga U-Zr-Nb revestido em Zircaloy e investigação da difusividade do urânio visando à estabilidade química do combustível”, DSc Thesis, CDTN, 120 p., (2015).
26. R. W. D. Pais and W B. Ferraz, “Estudo das Transformações de Fases nas Ligas U-2,5Zr-7,5Nb e U-3Zr-9Nb para Aplicação em Combustível Nuclear Avançado”, DSc Thesis, CDTN, 114p., (2015).
27. R. O. Elias and M. S. Dias, “Modelagem de Propriedades Térmicas de Ligas a Base de Zircônio e Urânio – Parte I: Pontos e Curvas de Referência”, Relatório de Iniciação Científica, CDTN, 17 p., (2014)
28. C.B. Basak, R. Keswani, G.J. Prasad, H.S. Kamath, N. Prabhu, “Phase transformations in U–2 wt% Zr alloy”, *Journal of Alloys and Compounds*, **471**, pp. 544-52, (2009).
29. C.B. Basak, “Microstructural evaluation of U-rich U–Zr alloys under near-equilibrium condition”, *J. of Nuclear Materials*, **416**, pp. 280–287, (2011).
30. M. Akabori, T. Ogawa, A. Itoh, A. and Y. Morii, “The lattice stability and structure of δ-UZr_2 at elevated temperatures”, *J. Phys.: Condens. Matter*, **7**, pp.8249-8257, (1995).
31. E.R. Boyko, “The Structure of the Phase in the Uranium-Zirconium System”, *Acta Cryst.*, **10**, pp. 712-713, (1957).
32. W. Chubb, “Physical properties of Zirconium-Uranium alloys”, pp. 78-88. IN: A.A. Bauer (ed), “An evaluation of the properties and behavior of Zirconium-Uranium alloys”, Battelle Memorial Institute, Report no. BMI-1350, 121 p., (1959)
33. A. Landa, P. Söderlind, P.E.A. Turchi, “Density-functional study of the U–Zr system”, *J. of Alloys and Compounds*, **478**, pp.103–110, (2009)
34. M. Anagnostidis, M. Colombia and H. Monti, “Phases metastables dans les alliages uranium-niobium”, *J. Nuclear Materials*,**11(1)**, p.67-76, (1964)
35. C. D’Amato, F.S. Saraceno and T.B. Wilson, “Phase transformations and equilibrium structures in uranium-rich niobium alloys”, *J. of Nuclear Materials*, **12(13)**, pp.291-304, (1964).
36. O.S. Ivanov and YU. S. Virgiliev, “The decomposition of the γ-uranium base solid solution as revealed by X-ray investigation”, *J. of Nuclear Materials*, **6(2)**, pp.199-202, (1962).
37. R.A. Vandermeer, “Phase transformations in a uranium + 14 at/% niobium alloy”, *Acta Metallurgica*, **28(3)**, p.383-393, (1980).
38. K. Andres, “Thermal Expansion of Alpha-Uranium below 10 K”, *Physical Review*, **170(3)**, p.614-7, (1968).

39. P. C. de Camargo, F. R. Brotzen and S. Steinemann, “Thermal expansion and elastic properties of Nb-Mo alloys”, *J. Phys. F: Met. Phys.,* **17**, p.1065-79, (1987).
40. J.W. Edwards, R., Speiser and H.L. Johnston, “High Temperature Structure and Thermal Expansion of Some Metals as Determined by X-Ray Diffraction Data. I. Platinum, Tantalum, Niobium, and Molybdenum”, *J. Applied Physics,* **22(4)**, p.424-8, (1951).
41. T.J. Heal, “The mechanical and physical properties of Magnesium and Niobium canning materials”, *Proc. 2nd. United Nations Int. Conf. on the Peaceful Uses of Atomic Energy, Geneva, 1-13/09/1958,* **5**, p.208-19, (1958).
42. T. Hüpf, “Density Determination of Liquid Metals”, *Technische Universität Graz,* http://portal.tugraz.at/portal/page/portal/Files/i5110/files/Forschung/Thermophysik/Thomas_Huepf_Dissertation.pdf, (2010).
43. P.M. Johnson, R.L. Lincoln and E.R. McClure, “Development of a high-temperature interferometric dilatometer using a laser light source”, *U.S. Bureau of Mines, Report of investigation 7142,* 13 p., (1968).
44. V.P. Lebedev, A.A. Mamalui, V.A. Pervakov, N.S. Petrenko, V.P. Popov, V.I. Khotkevich, “Thermal expansion of niobium, molybdenum and their alloy at low temperatures” (in Russian), *Ukrainskii Fizichnii Zhurnal,* **14(5)**, p.746-50, (1969).
45. A.P. Miiller and A. Cezairliyan, “Thermal Expansion of Niobium in the Range 1500-2700 K by a Transient Interferometric Technique”, *Int. J. of Thermophysics,* **9(2)**, p.195-203, (1988).
46. V. A. Petukhov, V. Ya. Chekhovskoi, V. G. Andrianova, A. G. Mozgovoi, “Experimental investigation into thermal expansion of some structural materials. niobium and niobium 5VMTs1 alloy”, *Teplofizika Vysokikh Temperatur,* **15(3)**, p.670-3, (1977).
47. A. Pialoux, M.L. Joyeux and G. Cizeron, “Étude du comportement du niobium sous vide par diffraction des rayons X à haute temperature”, *J. Less-Common Metals,* **87**, p.1-19, (1982).
48. W.J. Radcliffe, J.C. Gallop and J. Dominique, “A microwave method for thermal expansion measurement”, *J. Phys. E: Sci. Instrum.,* **16(12)**, (1983).
49. R. Roberge, “Lattice parameter of niobium between 4.2 and 300 K”, *J. Less-Common Metals,* **40**, p. 161-4, (1975).
50. D.J. Senor, J. K. Thomas and K.L. Peddicord, “Thermophysical property correlations for the niobium-1 % zirconium alloy”, *J. Nuclear Materials,* **173**, p.261-273, (1990).
51. T F Smith and T R Finlayson, “Thermal expansion of bcc solid solution alloys in the system Zr-Nb-Mo-Re”, *J. Phys. F: Metal Phys.,* **6(5)**, p.709-23, (1976).
52. M. E. Straumanis and S. Zyszczynski, “Lattice Parameters, Thermal Expansion Coefficients and Densities of Nb, and of Solid Solutions Nb-O and Nb-N-O and their Defect Structure”, *J. Appl. Cryst.,* **3**, p.1-6, (1970).
53. B.M. Vasyutinskiy et al., “High-temperature crystalline structure of Niobium and Vanadium”, *The Physics of Metals and Metallography,* **21**, p.134-5, (1966).
54. K. Wang and R. R. Reeber, “The role of defects on thermophysical properties: thermal expansion of V, Nb, Ta, Mo and W”, *Materials Sci. and Eng.,* **R23**, p.101-137, (1998).
55. G. K. White, “Thermal Expansion of Vanadium, Niobium, and Tantalum at Low Temperatures”, *Cryogenics,* **2(5)**, p.292-6, (1962).
56. R.A. Lopes Jr and M.S. Dias, “Specific Heat of the Uranium-Zirconium Alloys”, Relatório de Iniciação Científica, CDTN, 20 p., (2013).